

UNCLASSIFIED

AD NUMBER
AD871603
NEW LIMITATION CHANGE
TO Approved for public release, distribution unlimited
FROM Distribution authorized to U.S. Gov't. agencies and their contractors; Administrative/Operational Use; JUN 1970. Other requests shall be referred to Air Force weapons Lab., Kirtland AFB, NM.
AUTHORITY
AFWL ltr, 30 Nov 1971

THIS PAGE IS UNCLASSIFIED

AD871603

AFWL-TR-70-34

AFWL-TR-70-34

THERMAL SHOCK FRACTURE OF SINGLE CRYSTAL SILICON

Daniel N. Payton III
Capt USAF

David C. Straw
Capt USAF

TECHNICAL REPORT NO AFWL-TR-70-34

June 1970

AIR FORCE WEAPONS LABORATORY
Air Force Systems Command
Kirtland Air Force Base
New Mexico

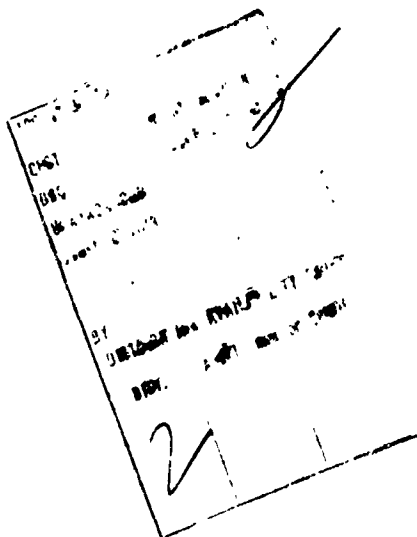
This document is the property of the Air Force Weapons Laboratory and is loaned to you for your information only. It is not to be distributed outside your organization without the approval of the AFWL-TR-70-34.

AIR FORCE WEAPONS LABORATORY
Air Force Systems Command
Kirtland Air Force Base
New Mexico

When U. S. Government drawings, specifications, or other data are used for any purpose other than a definitely related Government procurement operation, the Government thereby incurs no responsibility nor any obligation whatsoever, and the fact that the Government may have formulated, furnished, or in any way supplied the said drawings, specifications, or other data, is not to be regarded by implication or otherwise, as in any manner licensing the holder or any other person or corporation, or conveying any rights or permission to manufacture, use, or sell any patented invention that may in any way be related thereto.

This report is made available for study with the understanding that proprietary interests in and relating thereto will not be impaired. In case of apparent conflict or any other questions between the Government's rights and those of others, notify the Judge Advocate, Air Force Systems Command, Andrews Air Force Base, Washington, D. C. 20331.

DO NOT RETURN THIS COPY. RETAIN OR DESTROY.



AFWL-TR-70-34

THERMAL SHOCK FRACTURE OF SINGLE CRYSTAL SILICON

Daniel N. Payton, III
Captain USAF

David C. Straw
Captain USAF

TECHNICAL REPORT NO. AFWL-TR-70-34

This document is subject to special export controls and each transmittal to foreign governments or foreign nationals may be made only with prior approval of AFWL (WLIT), Kirtland AFB, NM, 87117. Distribution is limited because of the technology discussed in the report.

FOREWORD

This research was funded by the Laboratory Director's Funds No. 6142SS.

Inclusive dates of research were January 1968 through December 1969. The report was submitted 8 May 1970 by the Air Force Weapons Laboratory Project Officer, Captain Daniel N. Payton, III (WLET).

Information in this report is embargoed under the US Export Control Act of 1949, administered by the Department of Commerce. This report may be released by departments or agencies of the US Government to departments or agencies of foreign governments with which the United States has defense treaty commitments, subject to approval of AFWL (WLET), Kirtland AFB, NM, 87117.

The authors wish to thank V. R. Honnold, M. Peffley, C. Berggren, A. J. Goodman, A. Hoffland, C. Martin, and J. J. Wortman for discussion and technical assistance in these experiments.

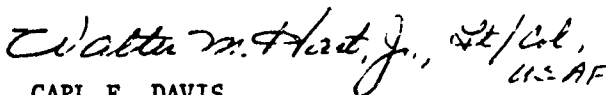
This technical report has been reviewed and is approved.



DANIEL N. PAYTON, III
Captain, USAF
Project Officer



JAMES E. SMITH
Major, USAF
Chief, Transient Radiation
Effects Branch


for CARL F. DAVIS
Colonel, USAF
Chief, Electronics Division

ABSTRACT

(Distribution Limitation Statement No. 2)

The usual approach to thermal shock fracture of crystalline material is the classic quenching of an initially hot crystal by subjecting it to a rapid cooling of its surroundings. A new approach can be obtained by the deposition of internal energy directly into the crystal by electron bombardment in an intense pulsed beam. If the sample thickness is chosen properly with respect to the range of the incident electrons in the material, a quite uniform deposition takes place minimizing the formation of shock waves. If the amount of energy deposited is sufficient, thermal shock fracture of the crystal occurs. A series of experimental investigations has been made by using high-speed photographic techniques. The results show values for crack initiation time and for crack tip propagation velocities consistent with thermal shock fracture.

AFWL-TK-70-34

This page intentionally left blank.

CONTENTS

<u>Section</u>		<u>Page</u>
I	INTRODUCTION	1
II	EXPERIMENTAL TECHNIQUE	6
III	RESULTS	10
	APPENDIX	
	A Partial Tabulation of Crack Length Data	21
	REFERENCES	24

ILLUSTRATIONS

<u>Figure</u>		<u>Page</u>
1	Reflection of a Compression Pulse at a Free Boundary	2
2	Behavior of a Thermal Shock Pulse	4
3	Schematic of Experimental Arrangement	7
4	Electron Energy Deposited in Silicon for Thermal Shock	11
5	Electron Energy Deposition in a Thick Sample of Silicon	12
6	Framing Camera Sequence of Silicon Fracture	14
7	Framing Camera Sequence of Silicon Fracture	15
8	Framing Camera Sequence of Silicon Fracture	16
9	Time-Dependent Crack Lengths from a Typical Crystal	18
10	Schematic Behavior of Crack Length in the Radial Oscillation Phase	19

SECTION I

INTRODUCTION

The fracture of solids upon the passage of shock waves has revealed an important new source of information about the fracture mechanisms and dynamic properties of these solids. A shock wave passing through a solid can produce fracture phenomena that can differ considerably from those produced under quasistatic loading. As is mentioned by Kolsky and Rader (Ref. 1), shock wave fracture differs from fracture produced under quasistatic loading in three important ways.

(1) Under quasistatic loading, the fracture develops from the single weakest point or flaw, and one consequently measures the tensile strength of the weakest flaw. In fracture produced by shock waves, the failure can nucleate at several points almost simultaneously as the shock wave passes.

(2) In brittle materials (such as silicon) the fracture almost invariably is nucleated at surface flaws under quasistatic loading so that the bulk tensile strength is closely related to the surface condition of the sample. The passage of traveling shock waves through the sample allows (by proper choice of sample shape) one to eliminate the role of the surface on the fracture phenomena.

(3) The tensile strengths of many solids depend markedly on the time of application of the stress and the duration of the stress pulse. Much is known about the detailed fracture behavior from the quasistatic loading times, but, for example, little is known about the rate effects on the tensile strength.

In the past few years considerable effort has been expended in studying the failure of materials under shock loading. Among these are the works of Rinehart and Pearson (Ref. 2), Schardin (Ref. 3), Berry (Ref. 4), and others (Ref. 5).

Fracture can be caused by the formation of a tensile wave when the normal shock compression wave interacts with and is reflected from a free surface. Schematically this is shown in figure 1. The compression wave is reflected at the free surface to form a tensile wave. As this tensile wave then progresses back through the sample it interacts with defects, which have lowered the local

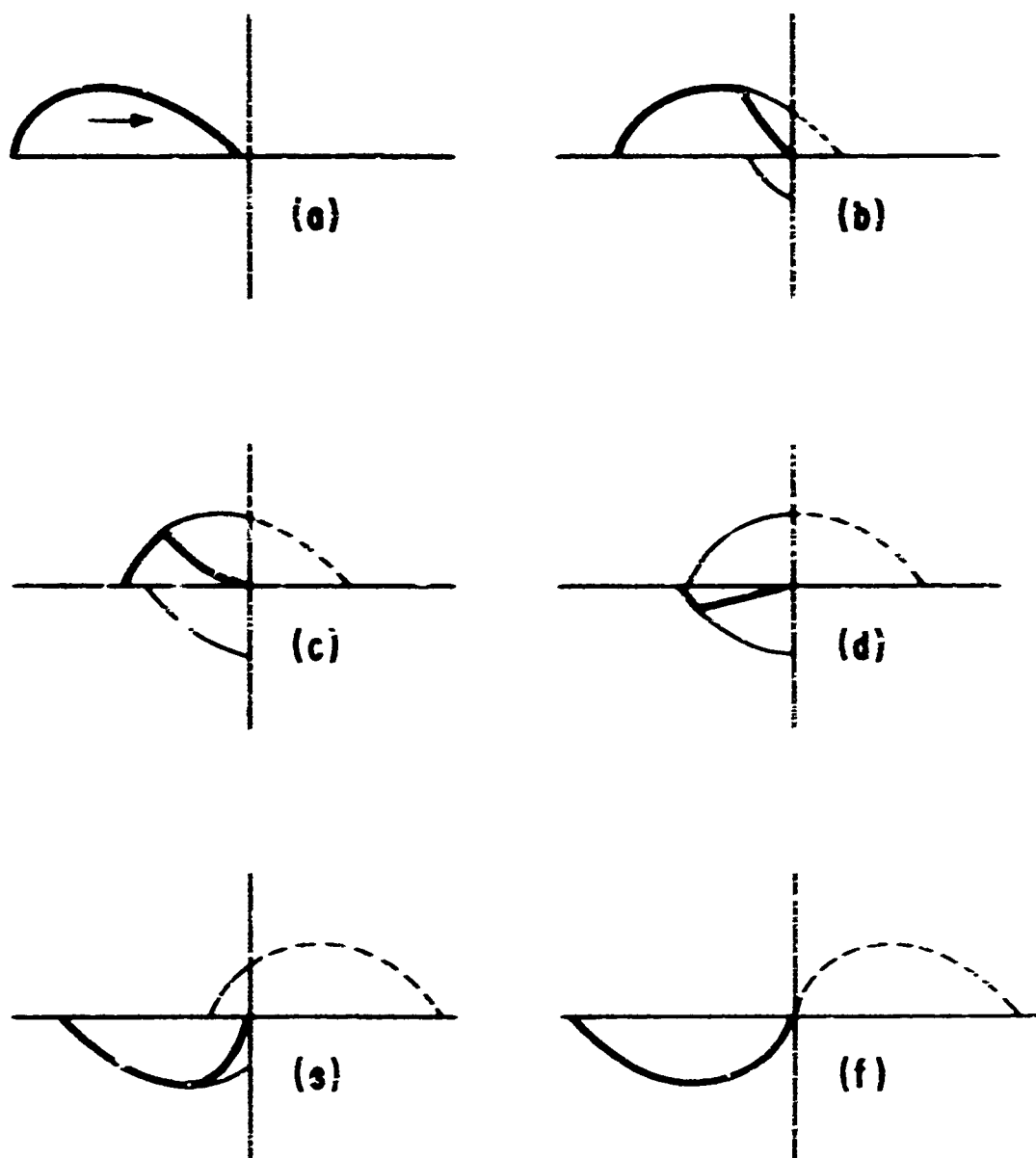


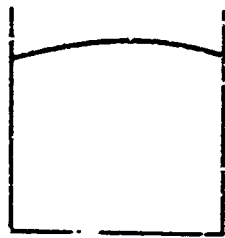
Figure 1. Reflection of a Compression Pulse at a Free Boundary

tensile strength enough that the tensile wave is able to create failure centers and cracks therefore propagate. If sufficient energy is not transferred from the wave to the defect center, the cracks may stop propagating after the wave has passed. The more brittle the solid the less this cessation of cracking occurs. In extremely brittle materials like single crystal silicon, catastrophic cracking usually occurs once a local tensile strength has been surpassed.

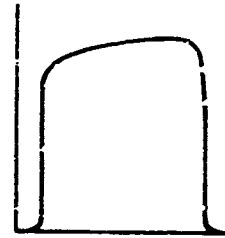
Fracture can also occur under shock conditions in which there is no moving compressional shock front. This is the phenomenon of thermal shock fracture. Thermal shock fracture occurs when an initially hot solid is rapidly quenched such that the rapid cooling causes the generation of tensile regions within the solid and in turn these tensiles interact with defects to form failure zones and allow fracture to occur. This is shown schematically in figure 2.

One method of studying thermal shock phenomena is to rapidly heat an initially cold solid internally to a high temperature. Thus, the solid suddenly finds itself at a higher internal temperature than its volume should allow and is effectively in a highly compressed state. As this internal compression is relieved, tensile "waves" are formed in the solid and the process of failure then proceeds from the local defects. In the case of the study of thermal shock in single crystal silicon, these defects are fewer in number and smaller in size than with noncrystalline or inhomogeneous materials. If a proper procedure for the uniform shock heating of single crystals of silicon can be found, one can then study the interaction of the defects with the tensile "waves" to form fracture, and furthermore one can then study the propagation of these cracks.

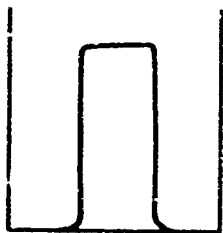
The use of an electron beam to deposit energy internally allows one to study the thermal shock fracture of small samples under closely controlled "quenching" conditions. The penetrating characteristics of high intensity pulsed electron beams allow one to study the thermal shock failure of small samples as well as the thermoelastic shock wave failure of thicker samples. To study the thermal shock failure of single crystal silicon, one must work with thin samples of silicon such that the range of electrons is long with respect to the thickness of the sample. In this case, the deposited energy will be relatively uniform over the thickness of the sample in the direction parallel to the electron beam. If, in addition, the lateral dimensions of the sample are chosen so that the flux of the beam across the sample is relatively uniform,



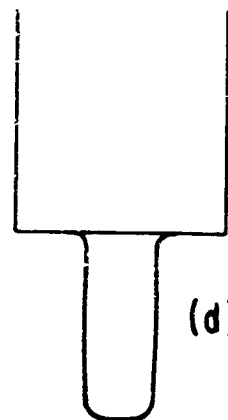
(a)



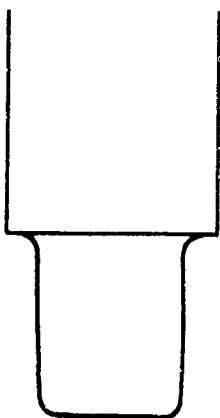
(b)



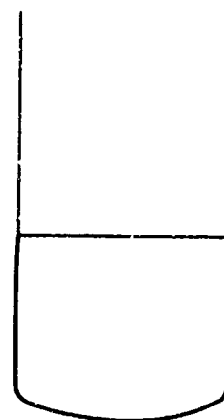
(c)



(d)



(e)



(f)

Figure 2. Behavior of a Thermal Shock Pulse

the deposition of electron energy will be relatively uniform throughout the sample. This report presents the use of this technique to study crack formation and propagation in single crystal silicon.

In this report we would like to present the first of a series of studies--experimental and theoretical--into the thermal shock fracture of single crystal silicon. To obtain accurate measurements of the time scales involved in the thermal shock fracture of silicon, we have observed the fracture of a large number of samples in a pulsed electron beam and have recorded these thermal shock fractures photographically. Section II describes the experimental techniques used; while Section III describes some of the results obtained. This study is the first part of an intensive investigation into fracture mechanisms. The experiments described in this paper are part of the experimental approach aimed at forming a testing ground for the theoretical investigation being performed concurrently.

SECTION II

EXPERIMENTAL TECHNIQUE

The most obvious approach when seeking the details of a mechanical event of microsecond time duration is that of high-speed photography. Because little is known about the actual order of events of a thermal shock fracture in a pulsed electron beam, the photographic approach seemed even more applicable because of the wealth of information to be obtained. Several important characteristics of the fracture such as fracture initiation time, crack-tip propagation velocity, and shock formation characteristics could be measured quantitatively from the film. This information along with the qualitative understanding gained from viewing the film gives one a better understanding of the mechanics of the fracture.

The experimental arrangement is shown in figure 3. The source of the pulsed electron beam is a commercially available machine, the Febetron 705.* The beam energy fluence is 20 cal/cm^2 at our working point with the electron energy spectrum having three predominant peaks at 2.2, 1.0, and 0.7 Mev. The electron beam energy is delivered with a full width at half-maximum of 50 nanoseconds. The beam delivered has an energy density that is uniform (within 10 percent) over a 2-cm diameter area at our working point.

The camera used for the principal part of this study was the Model 189 framing camera.** This camera uses a helium-driven rotating mirror that places the image, in turn, in 25 separate lens systems. This camera is capable of framing rates up to 4.2 million frames per second and delivers a sequence of 25 frames on conventional 35-mm film. The fact that the Model 189 is not a continuous-writing camera governs the event-triggering sequence. As seen in the schematic diagram of the experimental arrangement, figure 3, the camera triggers the lighting system and a delay trigger amplifier, which in turn triggers the electron beam. Consequently the complete event is initiated when the turbine (mirror) of the camera has reached the proper speed for the framing rate desired. This method of event triggering gives a precise record of the photographic exposure time and lapse time between exposures.

*Field Emission Corporation.

**Beckman and Whitley.

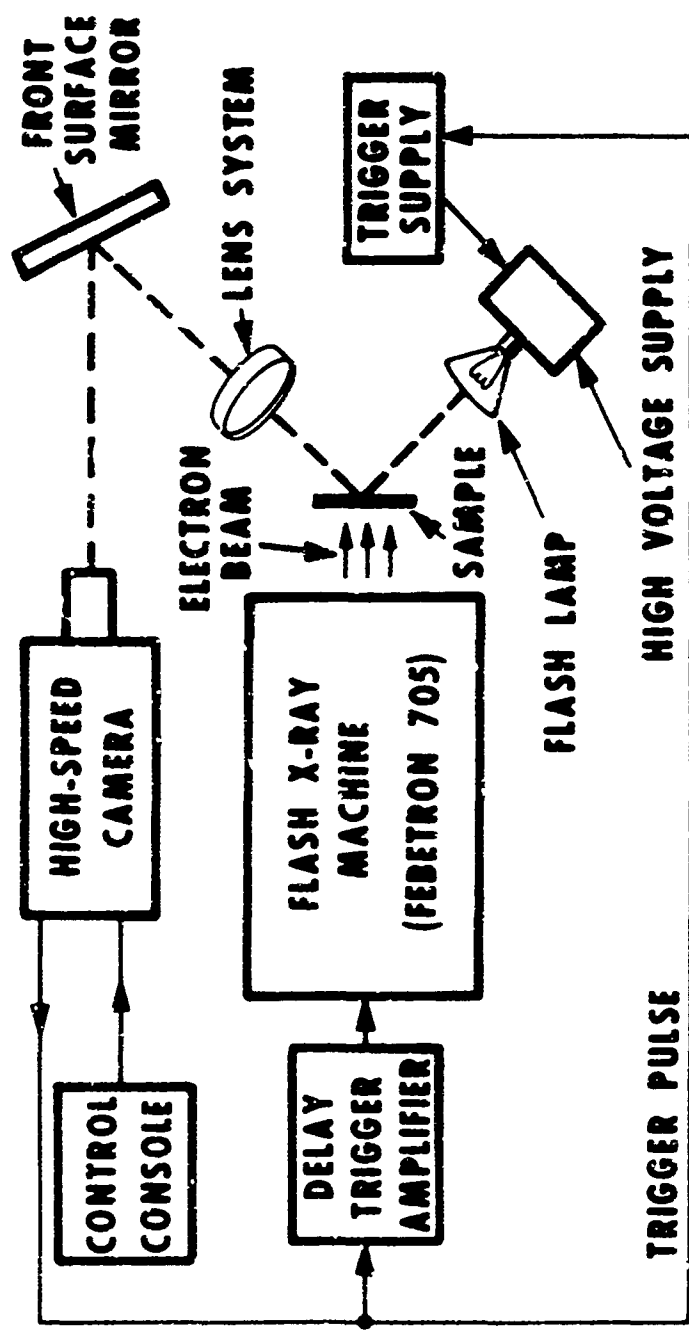


Figure 3. Schematic of Experimental Arrangement

A second camera has been used as a check and to achieve a better time resolution. This camera is an image converter camera,* which can deliver three photographs with exposure times as short as 5 nanoseconds with delays between exposures as short as 50 nanoseconds. The photographs taken with this camera supplement the information obtained with the Model 189 by increasing the time resolution.

The silicon crystals used were n-type single crystals with polished surfaces. The resistivity of the silicon used was 40 ohm-cm. After cutting to an approximate thickness of 0.5 mm, the surfaces were lapped and polished to remove the gross damage incurred in sawing and to provide an optical surface on the crystallographic plane of interest. The edges of the crystals were left rough so that many cracks eventually nucleated near these defect concentrations.

The light source was an xenon-filled flash tube that was pulsed with a silicon-controlled-rectifier (SCR) gated circuit. This light source consisted of two flash tubes** that delivered a light pulse of 13 megalumens with a full width at half maximum of 40 microseconds and a rise time to 90 percent of peak output of 12 microseconds.

By placing the crystal sample in the electron beam in an orientation such that the camera views the specular reflection of the light source, one can take advantage of the optical lever technique to detect small changes in the surface smoothness of the crystalline sample. This orientation has the advantage of allowing the use of lower speed films to record the event in a manner similar to back-lit shadow photography. In the majority of the photographs, the film used was Kodak Plus-X Panchromatic with an effective ASA film speed of 500, while in some cases a special recording film Kodak 2485 could be pushed to effective film speeds of approximately ASA 12,000 to record events when the reflecting surface was not polished. The resolution was approximately 26 lines/mm with Plus-X and dropped to approximately 16 lines/mm at the highest speed rating for Kodak 2485.

The recording framing rate found to be more desirable and most informative was a rate of two frames per microsecond. At this framing rate, the exposure time is 181 nanoseconds with a lapse time between frames of 319 nanoseconds

*TRW Instruments, Model 1D.

**General Electric, FT 220.

giving, for 25 exposures, a total writing time of approximately 12.5 microseconds. By timing the electron deposition to occur about 2 μ sec after the camera starts writing, one is left with about 10 μ sec of recording time to watch the initiation of cracks and their propagation across the crystal. It was found that within 10 μ sec all of the cracks had been formed and the crystal had begun to disintegrate.

The samples were suspended in the electron beam from a nylon mount. Nylon was chosen as the mounting material because it fluoresces strongly during the electron pulse, thereby giving an optical time mark for the energy deposition. The source of this strong fluorescence is a combination of Čerenkov radiation from the electron beam and stimulated emission from the electron absorption. This electrofluorescence has been discussed in detail elsewhere (Ref. 6). By observing this light emission in the photographs, one is able to measure to a reasonable degree of accuracy the time of energy deposition. This time is then considered the reference time for all later measurements. By using available data on the decay of the fluorescence, one can achieve an even more precise measurement of the times involved. This, however, is beyond the scope of the present work because of the lack of precision of other measurements, most notably the crack length measurements.

SECTION III

RESULTS

The most crucial test of the electron deposition technique for studying thermal shock phenomena is whether the deposition is sufficiently uniform over the sample volume to ensure that no shock waves are formed. If strong compressional shock waves are formed by the deposition of the electrons, all study of thermal shock fracture will be masked by propagating stress pulse. By using an electron deposition code called ELTRAN, the deposition has been calculated to be uniform within ± 12 percent over the 0.5-mm thickness of the silicon samples used. The restrictions to the validity of this calculation in this application occur because the technique underestimates long-range scattering and straggling losses and neglects the effects of space-charge buildup.

The result of a typical electron deposition calculation is shown in figure 4. One can see that the energy is quite uniform over the thickness of the sample and readily differs from the calculation of the energy deposition in a thick sample of silicon as shown schematically in figure 5. It is clear that the calculated initial conditions differ in the proper manner to give the difference between thermal shock and ordinary shock fracture as discussed. One would, however, expect some wave-like motion in the direction perpendicular to the electron beam (radial) because the uniformity of the flux is somewhat less than ideal. This conjecture is partially verified in the results to be discussed below. Further experiments that define more accurately the correlation between the state of thermal shock and ordinary shock have been completed. These will be published at a later date.

If strong shocks are formed in the crystal, one can make an estimate of the time of crack initiation. The sound velocity in single crystal silicon is on the order of 10 mm/ μ sec so that a sound wave can traverse the thickness of the crystalline sample many times each microsecond and acoustic disturbances normal to the beam axis can traverse the sample at least twice per microsecond. Consequently, if the fracture is stress induced by a longitudinally traveling shock wave, one would expect to see fracture initiation at extremely early times. This is not generally the result according to our observations. In

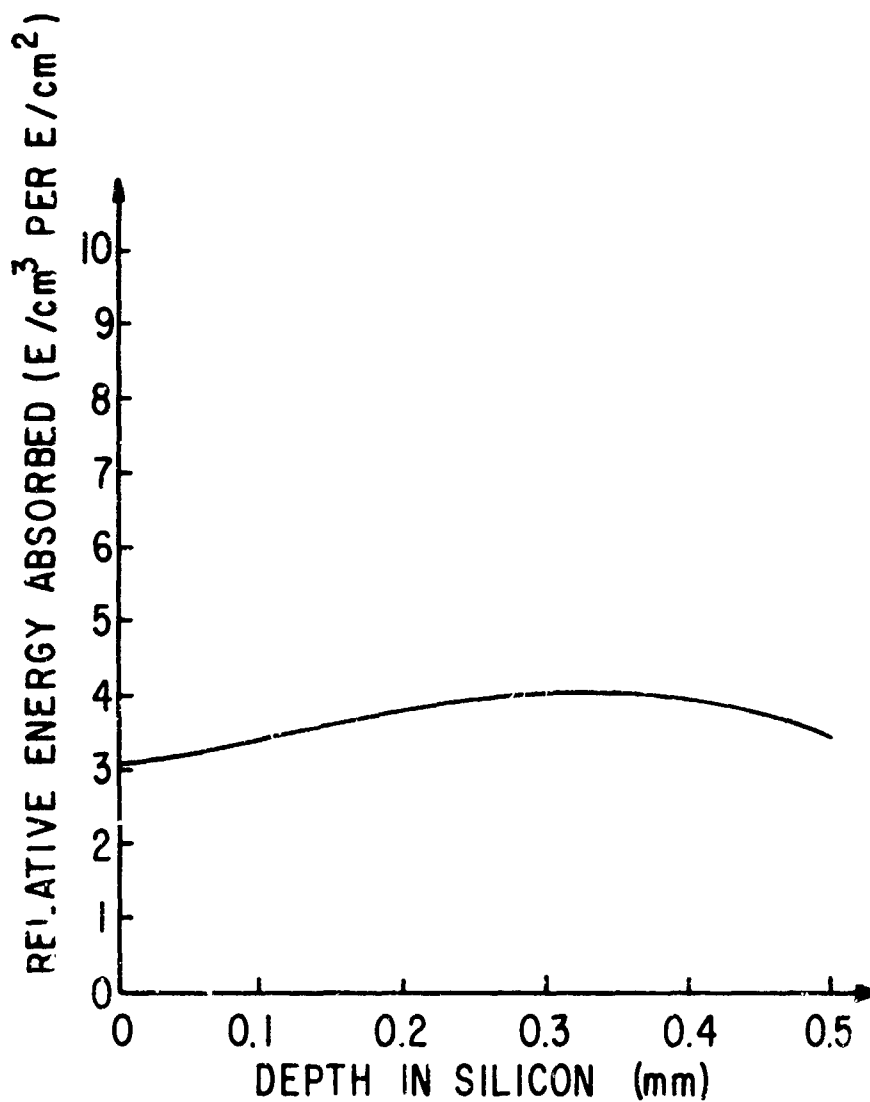


Figure 4. Electron Energy Deposited in Silicon for Thermal Shock

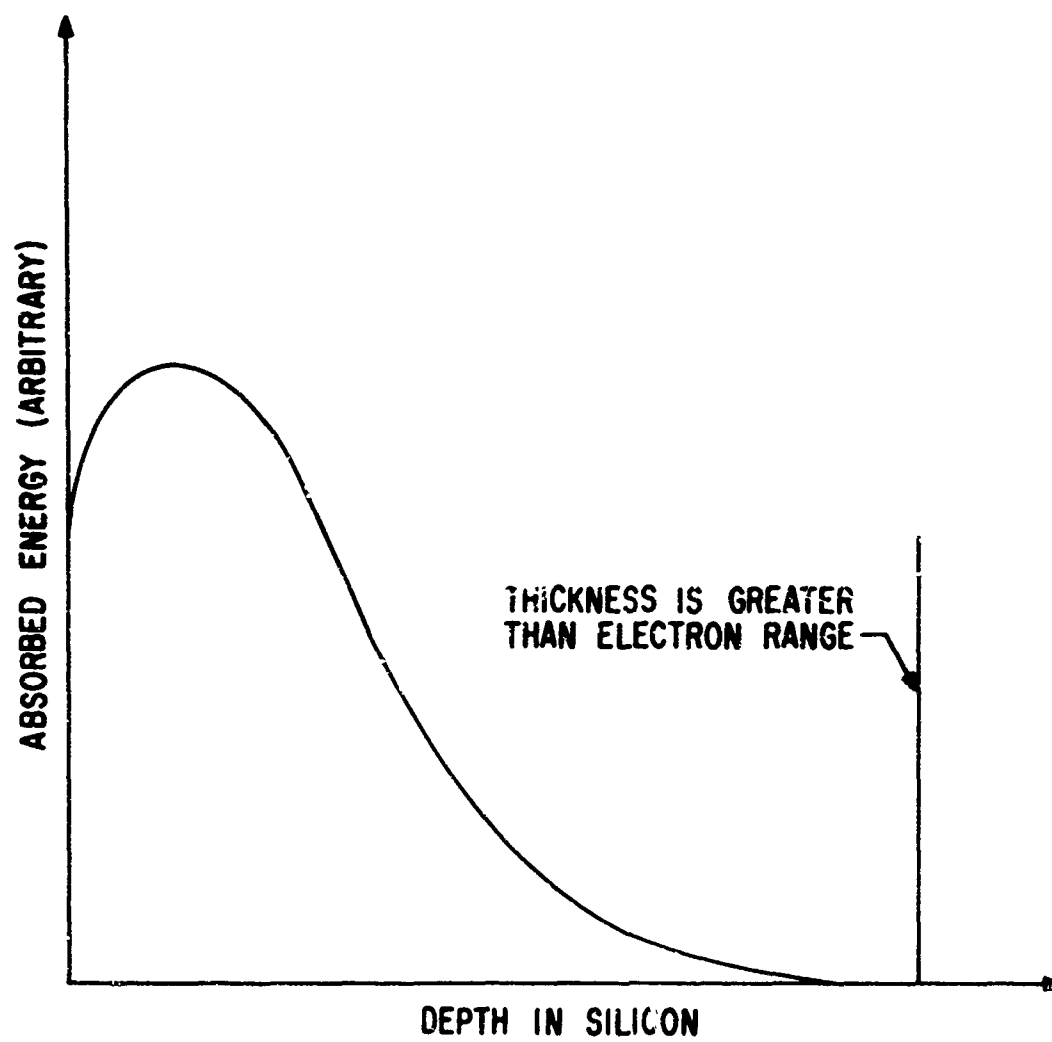


Figure 5. Electron Energy Deposition in a Thick Sample of Silicon

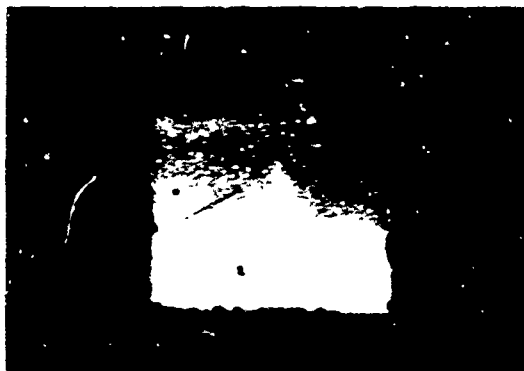
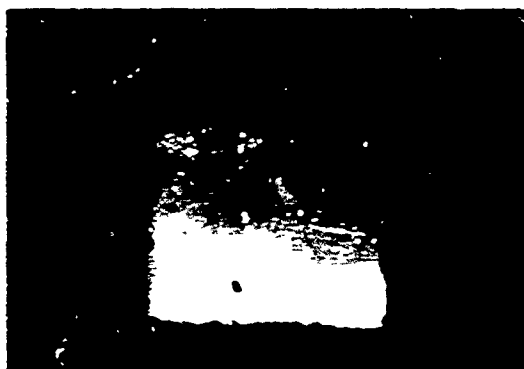
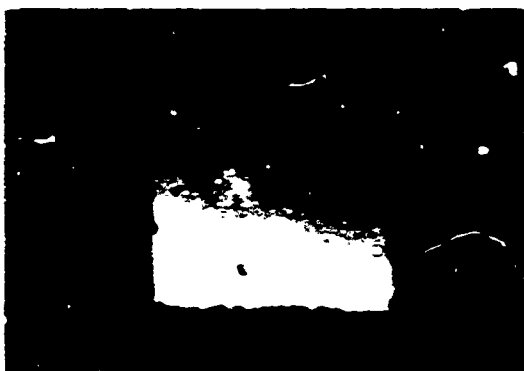
most examples of thermal shock fracture observed, the fracture initiated at times near 2 to 3 microseconds after the deposition occurred.

A series of photographic recordings was made for each of approximately 150 samples tested. From this series, a wealth of observational information about the fracture of single crystal silicon from thermoelastic pulses was obtained. Care must be taken not to draw excessively detailed conclusions from the photographic results. As in figure 6 the photographs show the intersection of the fracture and an exterior surface of the three-dimensional sample. One can measure only the projection of the propagating crack on the observed surface. However, it is clear that one can get limiting values for quantities such as the crack tip propagation velocity and crack initiation time. A further limitation is the finite resolution of the optical system involved. Thus the times measured from data similar to that shown in figure 6 are the times of appearance of the crack image on the photographic emulsion at the resolution limit. The time measurements differ consequently from reality by the time required for the crack to grow from nucleation to the discernable limit.

As in all high-speed photography with rotating mirror cameras, a shift of the location of image on the film plane is seen. This shift is caused by the finite moment arm between the reflection plane and the axis of rotation. This effect is readily calculable from geometrical considerations, but this calculation is unnecessary for the scope of this work because the magnification is unaffected by the field shift.

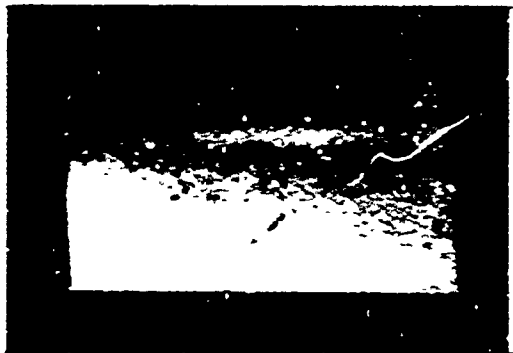
Figures 7 and 8 show two more examples of the data recorded. The orientation of each crystal is given on the figure. In figure 8 an interesting crack is seen to propagate irregularly from its nucleation center on the right edge of the crystal. Along this crack a small chip is seen to spall from the main crystal and oscillate as it moves away from the main crystal. This is seen as a rapid change in the brightness of that chip.

Measurements of crack length have been made from these photographs. Two methods of measurement have been used. In the first, an isodensity mapping of the photographic emulsion is made and measurements are taken from this mapping. This method of measurement is obviously more accurate, but it is extremely expensive to produce isodensity mappings. A second, more economical method of measurement was made by using a traveling micrometer eye-piece and low-power

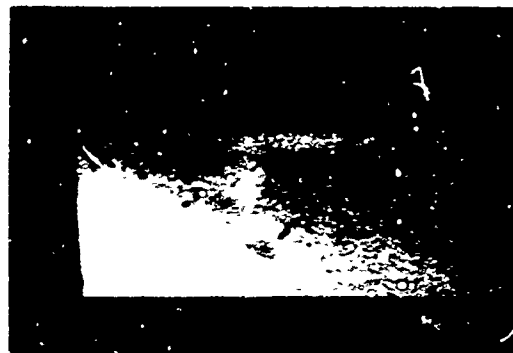


(Sample has been received by the Laboratory for analysis.)

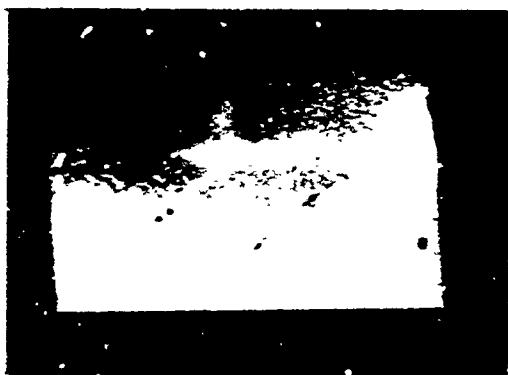
100-100000



$t = 2.5 \text{ sec}$



$t = 3.0 \text{ sec}$



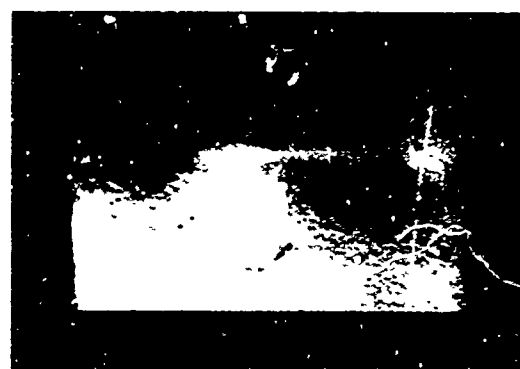
$t = 3.5 \text{ sec}$



$t = 4.0 \text{ sec}$



$t = 4.5 \text{ sec}$

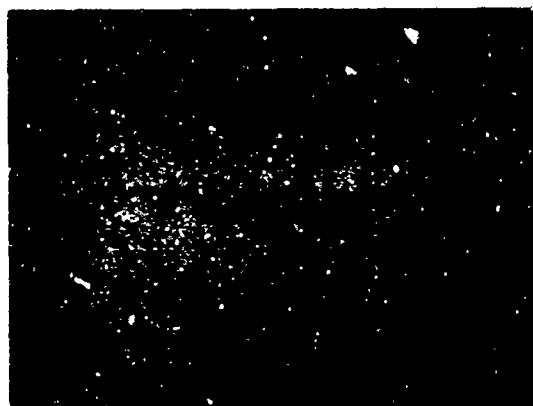


$t = 5.0 \text{ sec}$

Fig. 1. The process of the formation of a "fingerprint" fracture
(sample orientation is 0.10. Times are measured from energy deposition time.)



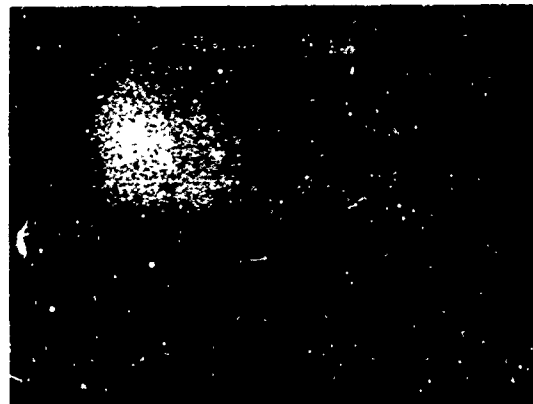
$t = 0.5 \text{ sec}$



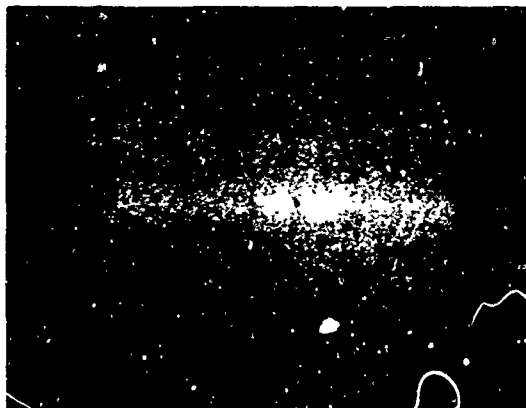
$t = 1.0 \text{ sec}$



$t = 1.5 \text{ sec}$



$t = 2.0 \text{ sec}$



$t = 2.5 \text{ sec}$



$t = 3.5 \text{ sec}$

Figure 8. Framing Camera Sequence of Silicon Fracture
(Sample orientation is (111). Times are measured from energy deposition time.
Note oscillating chip in lower right corner.)

microscope to measure the cracks on the original recording film. This method is potentially as accurate as the first and much more convenient.

The reproducibility of the fracture initiation time and the crack-tip propagation velocity was quite uniform over the series of samples studied. Examples of the crack length versus time for a typical sample are shown in figure 9. As can be seen, the initial crack opening velocity is approximately 1.5 mm/ μ sec as a measured lower limit because of the temporal resolution. This value can be low by as much as an order of magnitude because of the time resolution. The value obtained, however, probably exceeds the true crack propagation velocity because of the geometrical projections involved. The fact that these velocities are quite uniform and in the proper range of values seems to support the theoretical crack propagation velocity, which should be approximately 0.3 cm/ μ sec (Ref. 7).

From the examples shown in figure 9 an apparently confusing situation arises in which the cracks seem to shorten and then lengthen again. This comes from the transmission of acoustic-like pulses through the radial dimensions of the crystal causing the crack to open and close slightly. This phenomenon is observed in almost all of the samples tested. A plausible explanation of this opening and closing can be made by looking at the transit times for acoustic disturbances in samples of these dimensions. The acoustic velocity in the silicon is approximately 1 cm/ μ sec at normal pressure, consequently, in samples of 0.5-cm mean radial diameter, the periodic reinforcement of radially traveling compressive waves will occur approximately every 1 microsecond because the reinforcements will alternately be compressive and then tensile. The typical periodicity of these oscillations observed is approximately as shown schematically in figure 10. One notices a gradual change in the period after a few oscillations. This change may be caused by the relaxation of the crystal bulk and its effect on the acoustic velocity. A more detailed listing of some of the data obtained in this series of experiments is contained in the appendix.

A series of the photograph sequences has been assembled into motion picture form and is available from the author. This method of observing the data provides a new qualitative understanding of the processes involved in thermal shock fracture.

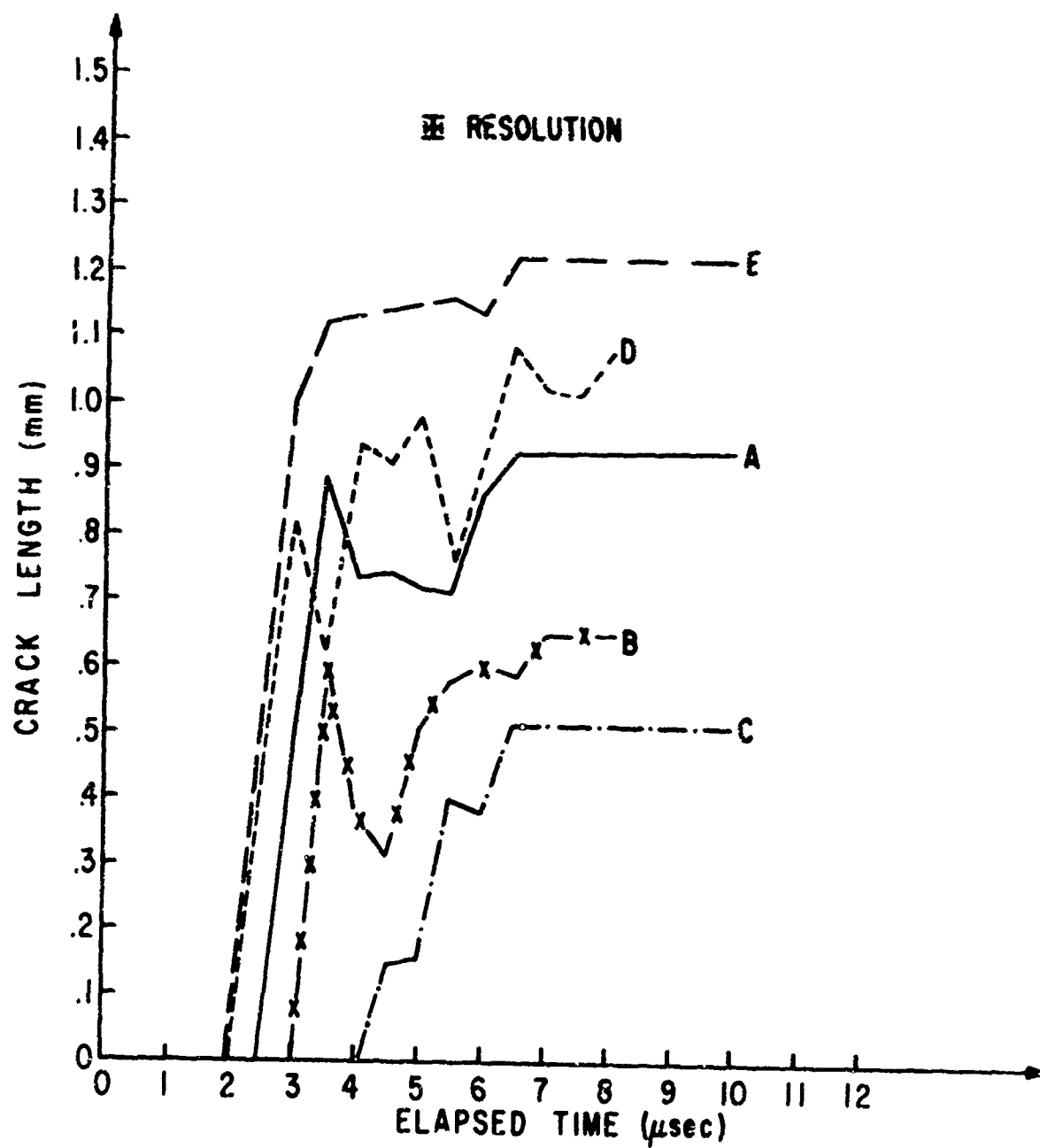


Figure 9. Time-Dependent Crack Lengths from a Typical Crystal

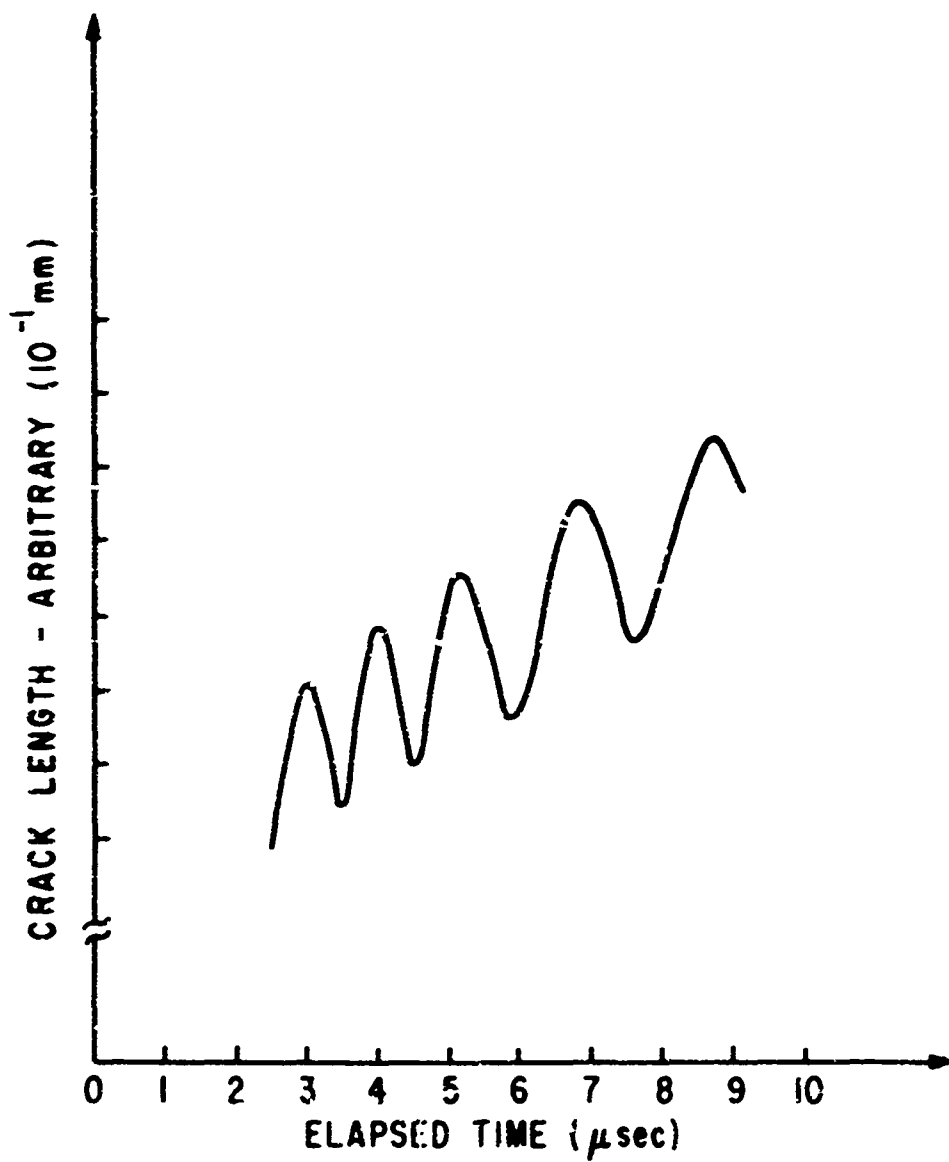


Figure 10. Schematic Behavior of Crack Length in the Radial Oscillation Phase

The observations of thermal shock fracture reported here differ from those reported by Oswald et al. (Ref. 8) in that our samples were quite small compared to the beam diameter and were thin compared to the range of electrons in silicon so that, as mentioned earlier, the deposition was quite nearly uniform. In the experiments of Oswald et al., the eventual fracture of the single crystal silicon was caused by the reinforcement of radially moving stress pulses in a large sample. Oswald's samples were thick enough to stop a major portion of the beam and were relatively large so that the lateral nonuniformity of the electron beam played an important role in the fracture.

The measurements reported here are the basis for more extensive work presently in progress. This work is aimed toward a clearer definition of the differences between thermal shock and ordinary shock.

APPENDIX

A PARTIAL TABULATION OF CRACK LENGTH DATA

<u>Corrected crack lengths* (mm)</u>				
<u>Sample No. 99</u>	Electron beam at t_o :			
Size: 4.9 x 4.97 x 0.5 mm	$t_o +$ (μ sec)	<u>A</u>	<u>B</u>	<u>C</u>
Framing rate: 1 frame/ μ sec	4	2.2	0.73	1.16
Orientation: (100)	5	4.04	3.08	2.21
	6	4.04	3.39	2.31
	7	4.04	4.75	2.29
	8	4.04	4.95	2.3
	20	4.04	4.95	2.3
<hr/>				
<u>Sample No. 102</u>	$t_o +$ (μ sec)	<u>A</u>	<u>B</u>	
Size: 4.9 x 4.94 x 0.5 mm	5	0.98		
Framing rate: 1 frame/ μ sec	6	2.29	0.67	
Orientation: (100)	7	2.51	0.77	
	8	2.63	1.07	
	9	2.66	1.07	
	10	2.66	1.07	
	20	2.66	1.05	
<hr/>				
<u>Sample No. 107</u>	$t_o +$ (μ sec)	<u>A</u>		
Size: 4.7 x 4.8 x 0.5 mm	4.0	0.9		
Framing rate: 2 frames/ μ sec	4.5	2.54		
Orientation: (100)	5.0	2.93		
	5.5	2.93		
	8.0	2.99		
<hr/>				
<u>Sample No. 130</u>	$t_o +$ (μ sec)	<u>A</u>		
Size: 4.5 x 4.7 x 0.5 mm	1.0	0.75**		
Framing rate: 2 frames/ μ sec	1.5	1.29		
Orientation: (111)	2.0	1.66		
	9.5	1.73		

*Corrected for apparent shortening of image due to perspective.

**Previously damaged.

Corrected crack lengths* (mm)Sample No. 131Electron beam at t_0 :

Size: 4.86 x 4.8 x 0.5 mm

Framing rate: 2 frames/ μ sec

Orientation: (111)

$t_0 +$ (μ sec)	<u>A</u>	<u>B</u>
2.0	1.29	0.18
2.5	1.54	0.79
3.0	1.54	0.81
3.5	1.54	1.14
9.5	1.54	1.14

Sample No. 135

Size: 4.85 x 4.85 x 0.43 mm

Framing rate: 2 frames/ μ sec

Orientation: (111)

$t_0 +$ (μ sec)	<u>A</u>	<u>B</u>	<u>C</u>	<u>D</u>
3.0	0.48	1.1	0.0	0.82
3.5	0.89	1.12	0.0	0.62
4.0	0.73	1.13	0.0	0.94
4.5	0.74	1.14	0.15	0.91
5.0	0.72	1.15	0.16	0.98
5.5	0.71	1.16	0.4	0.77
6.0	0.86	1.14	0.38	0.94
6.5	0.92	1.22	0.51	1.09
8.0	0.93	1.22	0.51	1.08

Sample No. 140

Size: 2.67 x 3.06 x 0.5 mm

Framing rate: 2 frames/ μ sec

Orientation: (111)

$t_0 +$ (μ sec)	<u>B</u>	<u>C</u>	<u>E</u>	<u>J</u>
1.0	0.0			
1.5	0.57			0.5
2.0	0.6	0.0	0.54	0.79
2.5	0.68	0.0	0.9	0.97
3.0	0.72	0.09	0.7	0.71
3.5	0.59	0.12	1.23	1.31
4.0	0.56	0.0	1.22	0.0 ?
4.5	0.55	0.24	1.1	1.23
5.0	0.63	0.0	1.31	0.95
5.5	0.63	0.19	1.3	0.89
6.0	0.59	0.24	1.18	0.65
6.5	0.61	0.24	1.36	1.09
7.0	0.67	0.24	1.3	1.07
7.5	0.65	0.24	1.48	1.02

*Corrected for apparent shortening of image due to perspective.

<u>Corrected crack lengths* (mm)</u>				
<u>Sample No. 142</u>		Electron beam at t_0 :		
Size: 2.27 x 2.98 x 0.5 mm	$t_0 +$			
Framing rate: 2 frames/ μ sec	<u>(μsec)</u>	<u>A</u>	<u>B</u>	<u>C</u>
Orientation: (111)	1.0	0.28	0.0	0.0
	1.5	0.81	0.0	0.0
	2.0	1.03	0.33	0.15
	2.5	1.06	0.55	0.54
	3.0	1.02	0.71	0.94
	3.5	1.33	0.71	0.9
	4.0	1.1	0.74	1.52
	4.5	1.18	0.74	0.88
	5.0	1.26	0.74	1.52
	5.5	0.97	0.74	1.34
	6.0	1.2	0.74	1.58
	6.5	1.4	0.74	1.01
	7.0	1.24	0.74	1.44
	7.5	1.25	0.74	1.55
	8.0	1.24	0.74	1.54

*Corrected for apparent shortening of image due to perspective.

REFERENCES

1. Kolsky, H., Rader, D., Fracture: An Advanced Treatise, Vol I, H. Liebowitz, Ed., Academic Press, New York, 1968.
2. Rinehart, J. S., Pearson, J., Behavior of Metals under Impulsive Loads, Dover, New York, 1965.
3. Schardine, H., Fracture, B. L. Averbach, D. K. Felbeck, G. T. Hahn, D. A. Thomas, Eds., Wiley, New York, 1959.
4. Berry, J. P., Fracture Processes in Polymeric Solids, B. Rosen, Ed., Wiley, New York, 1964.
5. Fracture: An Advanced Treatise, Vols I through VII, H. Liebowitz, Ed., and references contained therein, Academic Press, New York, 1968.
6. Payton, D. N., III, Straw, D. C., "Electrofluorescence of Polymeric Solids," Bull. Amer. Phys. Soc. Ser II, 14, 1969.
7. Hanson, M. E., Sanford, A. R., Dynamic Tensile Fracture, New Mexico Institute of Mining and Technology, Report T-965, 1969,
8. Oswald, R. B., Jr., Schallhorn, D. R., Eisen, H. A., "Laser Interferometric Determination of the Dynamic Response of Solids," IEEE Transactions on Nuclear Science NS-15, 1968.

14 KEY WORDS	LINK A		LINK B		LINK C	
	ROLE	W*	ROLE	W*	ROLE	W*
Thermal shock Fracture Silicon Electron Thermoelastic response High-speed photography						

UNCLASSIFIED

Security Classification

DOCUMENT CONTROL DATA - R & D

Security Classification of this data is shown and indicating any other restrictions on the report, if applicable

1 ORIGINATOR'S REPORT NUMBER Air Force Weapons Laboratory (WLET) Kirtland Air Force Base, New Mexico 87117		2 ORIGINATOR'S REPORT NUMBER UNCLASSIFIED	
3 REPORT TITLE THERMAL SHOCK FRACTURE OF SINGLE CRYSTAL SILICON			
4 DESCRIPTION OF REPORT Type of report and inclusive dates January 1968-December 1968			
5 AUTHOR(S) (Last name, first name, middle initial, last name) Daniel N. Payton, III, Captain, USAF; David C. Straw, Captain, USAF			
6 REPORT DATE June 1970	7 ORIGINATOR'S REPORT NUMBER 30	8 ORIGINATOR'S REPORT NUMBER 8	
9 CONTRACT OR GRANT NO.	10 ORIGINATOR'S REPORT NUMBER AFAL-TR-70-34		
11 PROJECT NO. Lab Dir Funds, No. 6143SS	12 ORIGINATOR'S REPORT NUMBER This report		
13 DISTRIBUTION STATEMENT This document is subject to special export controls and each transmittal to foreign governments or foreign nationals may be made only with prior approval of AFWL (WLET), Kirtland AFB, NM, 87117. Distribution is limited because of the technology discussed in the report.			
14 SUPPLEMENTARY NOTES		15 ORIGINATOR'S REPORT NUMBER AFWL (WLET) Kirtland AFB, NM 87117	
16 ABSTRACT (Distribution Limitation Statement No. 2) The usual approach to thermal shock fracture of crystalline material is the classic quenching of an initially hot crystal by subjecting it to a rapid cooling of its surroundings. A new approach can be obtained by the deposition of internal energy directly into the crystal by electron bombardment in an intense pulsed beam. If the sample thickness is chosen properly with respect to the range of the incident electrons in the material, a quite uniform deposition takes place, minimizing the formation of shock waves. If the amount of energy deposited is sufficient, thermal shock fracture of the crystal occurs. A series of experimental investigations has been made by using high-speed photographic techniques. The results show values for crack initiation time and for crack tip propagation velocities consistent with thermal shock fracture.			

DD FORM 1473
1 NOV 63

UNCLASSIFIED

Security Classification